Complex small pelagic fish population patterns arising from individual behavioral responses to their environment

Supplementary Information

Brochier et al.

Contents

Supplementary Tables

Supplementary Figures

1 - Supplementary Method

1- Overview, Design concepts, Details of Evol-DEB model

We have developed a biophysical model linking processes at different scales: physical and biogeochemical regional dynamics (ROMS-PISCES 3D simulation of the upwelling system), larval dispersion, fish dynamic energy budget (DEB) and swimming behavior. This model, hereafter called "Evol-DEB", was developed in Java from the codes of the models Ichthyop (Lett et al. 2008) and Evol (Brochier et al. 2009). The model description follows the ODD (Overview, Design concepts, Details) protocol (Grimm et al. 2006; 2010).

1.1. Purpose

This model was built to explicitly represent the spatial population dynamics of *S. aurita* in western African waters in order to make the model's predictive skills useful for management purposes. Indeed, the potential impact of spatial management plans can be assessed with this model, as well as the impact of past climate variability and future climate change, providing that forcing data are realistic enough. The presented approach is intended to be generic and hence can be applied to small pelagic fish species in other regions if sufficient information is available.

1.2. Entities, state variables, and scales

Fish individuals and the environment are the two entities taken into account by the model. The model is mono-specific and thus individuals represent *S. aurita* fish micro-cohorts, hereafter designed as super-individuals. The state variables for these entities are the age, the spatial coordinate, and the three state variables needed to describe the energy levels which are reserve, structural volume and maturity or reproduction buffer. The formalism used to represent these variables follows Dynamic Energy Budget theory (DEB; Kooijman, 2010). Other variables like fish length, weight and eventually number of eggs spawned can be derived from these DEB variables. All variables are updated every hour depending on experienced environment and, when appropriate, spawning activity. Each super-individual (SI) initially represents a number of eggs passively advected by currents. Depending on environmental conditions, eggs will hatch and larvae will grow, and once individuals are able to swim, the SIs move following oriented (or directed) swimming, considering that all individuals of the same cohort remain in schools, or that they cluster and spawn together (cluster-microcohort equivalence theory; Lefur et al. 2009) and experience the same mortality rates (see Section 2.3). The whole *S. aurita* population in West Africa is estimated by acoustics to less than 10 million tons. The number of SIs was set as a trade-off between computing capabilities and the need to get reproducible model outputs. The stochasticity tests showed that ~1000 super-individuals were enough to get similar model outputs between two realizations of a simulation (mean changes in biomass distribution <2%). In order to divide the whole population into at least 1000 super-individuals, we need them to represent each a maximum biomass of ~10000 tons (Fig. S 1). The maximum number of eggs per SI was set to 10^{10} so that with average temperature and food conditions, and with natural mortality rates, the biomass of the mature SI peaks remain at ~10000 tons. The question of the radius, or volume, associated with the SIs is complex since it involves the numbers of fish represented, their body-length, local density, spawning behavior, diurnal behavior, and other environmental factors. Here we reduce this complexity by considering the SI biomass to be evenly distributed in the cells of the hydrodynamic model (~8x8km), corresponding to a maximum biomass of 156 tons/km^2 for one SI. The SIs also record their date and place of birth and the temperature and salinity that occur at this time and place, a memory that can be later used for the habitat preferences and spawning strategy (see Design Concepts; Section 1.4).

The environment (currents, temperature, salinity and plankton carbon biomass) is described by the output of a coupled physical-biogeochemical simulation as archived 4D-gridded data (3 spatial dimensions plus time) (see

Section 1.6.2).

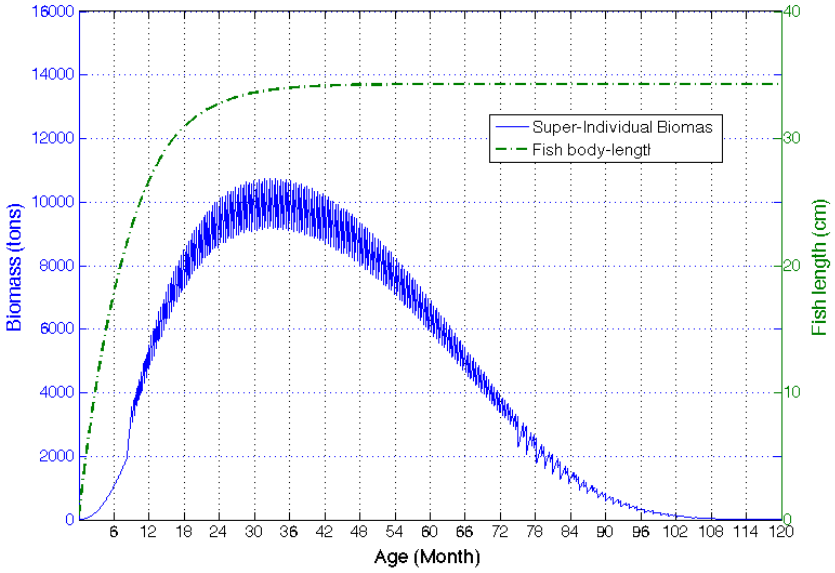

Fig. S 1: Fish growth (length in cm) and change in biomass represented by a super-individual in the case of a constant environment (f=0.8, T = 18°C). The oscillations of the biomass correspond to spawning events.

1.3. Process overview and scheduling

For each time-step, the environment is updated by interpolating the corresponding data from the daily archived ROMS-PISCES simulation. Time is discrete with time-step set to 1h. This time-step has to be chosen such that in a single time-step, individuals cannot cross strong environmental gradients; *i.e.*, they cannot cross more than two cells of the hydrodynamic model grid. A time-step of one hour allows individuals to rapidly re-adjust their swimming trajectory and avoid being transported offshore of the upwelling food-rich area. The maximum speed for *S. aurita* schools ranges ~10 km/h for adults, and the grid resolution we used was ~8 km so that a 1h time-step was appropriate. However, studying the effect of finer physical structures on the fish movement would require a finer spatial grid together with a smaller time-step. Once the environment is updated, a loop over each super-individual (SI) is performed. For each SI, the following actions are taken in this order: (1) age and position are updated; (2) the number of fish represented is updated (birth, mortality); (3) the energy budget is updated, with consequences on growth and maturation; and (4) if conditions are met, one spawning event every 24h. These processes are illustrated in the following flow chart and are detailed hereafter.

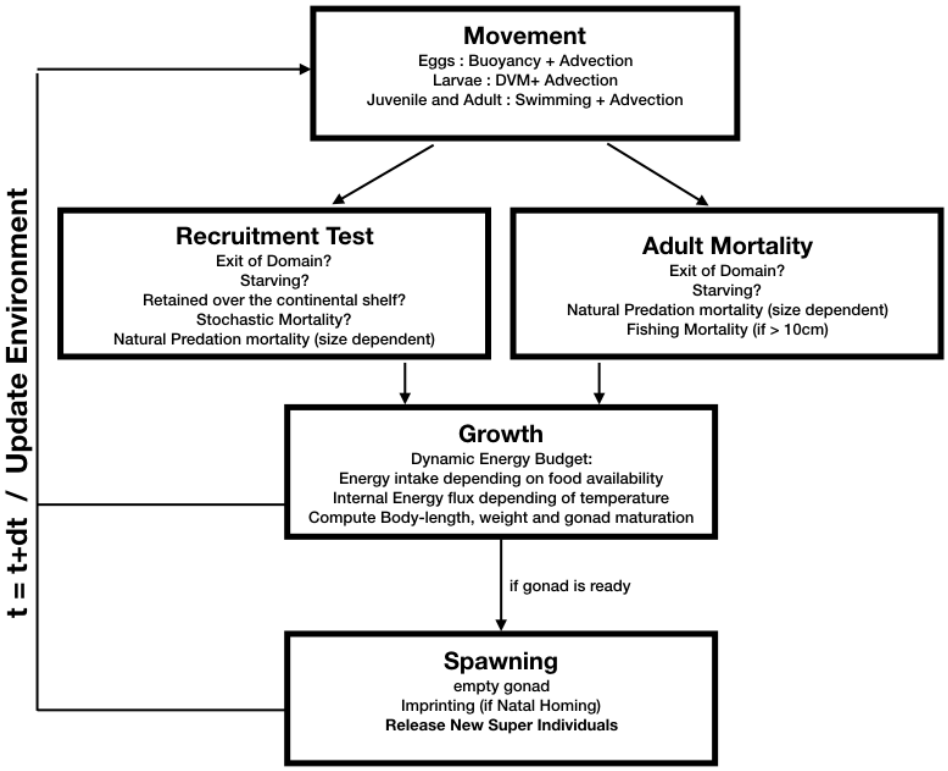

1.3.1 Position update

Eggs and larvae are passively transported by horizontal of currents. During the egg stage, positive buoyancy is applied. From hatching and until the yolk-sac has been absorbed, neutral buoyancy was applied. Afterwards, diurnal vertical migrations are performed between the surface and 50m depths. These settings were arbitrarily chosen because of the lack of observational data; however, their variability did not affect strongly the retention in the Senegalese and Mauritanian nursery area (Mbaye et al. 2015). After the yolk-sac has been absorbed, the horizontal swimming ability progressively develops, with a speed proportional to the body length. Horizontal swimming was modeled with an extended kinesis algorithm adapted from Okunishi et al. (2012) and Watkins et al. (2013). This algorithm combines fish velocity at the previous time step (inertial component), and a random component with a relative weight depending on the Habitat Quality Index (HQI; see Section 1.7.3 below) experienced by the fish. If the habitat improves, the fish continues in the same direction, otherwise it may turn in a random direction (but still with an inertial component; see Submodels, Section 1.7).

1.3.2 Update the number of fish per super-individual: applying Mortality.

Two mortality functions are applied in the following order: exit of the domain, starvation and simultaneously: predation, fishing and senescence. At this stage, no intraspecific competition was included in the model. The details of the mortality functions are given in Submodels (Section 1.7.2).

1.3.3 Update the energy budget: growth and maturation.

The energy budget is updated at each time step according to food and temperature experienced by the fish at its current location. The body-length, the weight and the maturity are derived at each time-step from the energy budget (Section 1.7.3). Once an individual is mature, the energy is allocated directly to gonad maturation and spawning occurs each time the gonad is mature. Ideally, the duration of the passive, early life stage should also be determined by the energetic budget of the growing larvae, itself relying on temperature and food availability (see Section 1.3.4). However, the current version of the *S. aurita* bioenergetics model during the early life stage under-estimated the egg and larval duration; hence, we applied a fixed duration for egg (1 day) and yolk-sac larvae (8 days) following Mbaye *et al.* (2015).

1.3.4 Newly spawned individuals

When individuals are ready to spawn according to the bioenergetic model, a number of new SI of age-0 (eggs) are released at the location of the SI spawners. The spawning frequency depends on the energy flow toward gonad maturation at each time step (according to temperature and food availability). The number of super-individuals released is such that each one may account for a maximum number of 10^{10} eggs, corresponding to a spawning biomass of 2.5 tons given a relative fecundity of 400 eggs/g (Fréon, 1988). In optimal conditions, the maximum spawning frequency was set to one per 24h, according to field observations by Fontana et al. (1969).

1.4. Design concepts

1.4.1 Basic principles

The model design relies on a set of three main theories that encompass the larval survival conditions, the bio-energetic budget and the natal homing behavior.

For the larval survival, we take advantage of the conceptual framework of Bakun's triad which states that in upwelling areas, recruitment relies on enrichment (from the upwelling), retention of larvae in rich areas, and concentration of their food in patches (Bakun, 1996). The bioenergetic budget of the individuals was computed using a dynamic energy budget (DEB) model (Kooijman, 2001). In the DEB model, different combinations of food availability and temperature that can lead to similar growth curves.

Mullon et al. (2002), and later Brochier et al. (2008) explored the generalized natal homing behavior for small pelagic fish with an earlier version of the present model, based on geographical memory assumptions. Here we considered a softer natal homing definition, considering it only affects the temperature preference for the definition of the HQI (combined with the food functional response, Eq. 5). Following the bioenergetic model, targeting warm waters where food is not limiting or colder water with less food can both lead to acceptable living conditions. Within the temperature ranges where *S. aurita* are observed, 10-30°C, there is room for both strategies.

Finally, the complexity expanded in the model is an interplay between (1) fish preconditioning to spawning, *i.e.,* temperature and food abundance level experienced by mature individuals, and (2) early life stages history. The combination of both might largely determines the success of reproduction, and hence the population dynamics. The implemented homing behavior links the two stages (preconditioning and early life) by the fact that adults tend to expose their offspring to similar early life histories they experienced and that resulted in successful conditions for themselves. The purpose of the study is to understand how these basic principles interplay in generating the observed population spatial dynamics, in particular the seasonal migration patterns.

1.4.2 Emergence

The entire population's dynamics emerges from the adaptive behaviors of the individuals. Population characteristics emerging from the model can be divided in two categories:

(a) patterns that can be compared with observations, mainly the biomass seasonal and inter-annual variability in the country where it has been monitored. Individual fish histories such as trajectories, variability of condition factors are also an emerging outputs that can be compared to observations, notably to fish histories reconstructed from otolith analysis. However, such analyses were not carried out yet, so that simulated individuals' trajectories still fall in the second category:

(b) patterns that emerge from the model for which no observations are available for comparison purposes. In particular, this is the case for the relative contribution of the different nursery areas to (1) the overall recruitment, (2) the seasonal migration patterns, and (3) the inter-annual fluctuations of the population. The relative contribution of the different nursery areas have important implications for population connectivity but can be validated only indirectly (through validation of the former population characteristics).

1.4.3 Adaptation

Individuals adapt their swimming and spawning behavior according to the environment, their age and their life history. Their swimming behavior leads them toward an environment that is a good trade-off between the distance to the preferred temperature and the level of food availability. In that sense, this trait seeks for increasing the "well-being" of the individuals, the ideal environment being the exact preferred temperature with abundant food.

1.4.4 Fitness

The preferred environment was selected in order to maximize the "fitness" as a trade-off between the chance of survival of the offspring and the energy intake by the adult. Following its co-occurrence with abundant food and retention areas, the individual temperature preference may lead to more or less successful reproduction events, *i.e.*, spawning and survival of the individuals until maturity. Thus, after a few generations, the temperature preference distribution among the total population may maximize the average fitness of the population. As a consequence, interannual variability in hydrodynamics, such as upwelling intensity, affects the population fitness and thus is responsible for population abundance variability.

1.4.5 Learning

There is no learning at the individual level. However, at the population level, there is a natural selection of the suitable temperature distribution for spawning. Indeed, individual spawning in temperatures beyond the limit for successful reproduction rapidly disappear from the population (see Initialisation; Section 1.5).

1.4.6 Sensing

Individuals perceive their environment through the temperature and food concentration at their location. The HQI is derived from these and from the individuals' temperature preference and tolerance. The temperature preference corresponds to the individuals' natal temperature (see Basic principles*;* Section 1.4.1). The temperature tolerance

was set as an increasing function of fish age; *i.e.*, older fish may seek food in a wider range of temperature than young fish (Fig. S1).

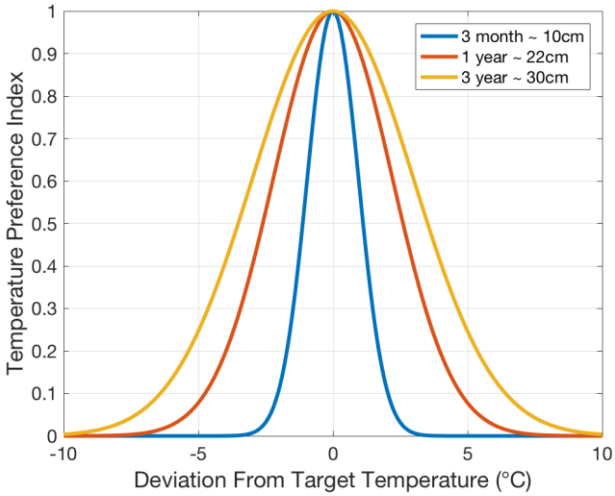

Fig. S 2: Temperature preference index according to deviation from target temperature at 3 months (~10cm, blue line), 1 year (~22cm, red line) and 3 years (~30cm, yellow line). Body length at age was estimated using a von Bertalanffy model with parameters from Freon (1988).

1.4.7 Stochasticity

Stochasticity is present at initialization, since the initial distribution of age-0 super-individuals is random along the continental shelf. Stochasticity also appears in the swimming algorithm, through random parameter of the kinesis algorithm (see Section1.7.2). The third source of stochasticity is in the recruitment process. Indeed, each day, a maximal number "*N_rec*" of new pre-recruited SI (*i.e.*, SIs with age > 30, retained over the continental shelf) was allowed. Thus, if for a given day more than *N_rec* SIs reach age 30 and satisfy to the shelf retention criterion, a random selection is done to select the *N_rec* SIs that will continue in the simulation, while the other ones are removed. Note that for each candidate pre-recruited SI the random selection was weighted by a value proportional to the continental shelf width at its location. This allowed compensating for the lower retention rates generated by the hydrodynamic model over the continental shelf due to coarse resolution (Mbaye et al., 2015).

1.4.8 Collectives

The fish remain within a given super-individual but no collective behavior between super-individuals was included in the model. Super-individuals spawned at the same place and time are likely to have a similar spatial behavior, *e.g.*, following the same food patches, but the random components in the swimming algorithms and the variability of oceanic features (at mesoscales for instance) may induce a divergence in the trajectories resulting in life histories that can differ significantly.

1.4.9 Observation

The growth and trajectory data for each SI are recorded each month (or finer time step if needed): longitude, latitude, age, number of individuals, the four state variables of the DEB, and an identification number. Furthermore, the complete list of SI is recorded with the data of both natal and recruitment environment: longitude, latitude,

temperature, date, and identification number. In the post-processing of these records we reconstruct (1) the fish biomass recruited to fisheries over the continental shelf in the different fishing areas, (2) the spawning patterns, (3) the fish condition factor, (4) the mean swimming direction, and (5) the relative contribution of the different nursery areas to the total population.

1.5 Initialisation

During the first year of the model run, 10 new super-individuals of age 0 (representing 10^{10} eggs each) were released each day at a random location of the continental shelf (bathymetry<200m) between 11°N to 30°N. This led to the release of 3650 SIs during the first year. It appeared to be sufficient to seed the environment with this species in our mono-specific model. Model outputs are analyzed after 10 years of spin-up, *i.e.,* more than twice the maximum *S. aurita* life time in the model (4.5 years, see Section1.7.7), so that the population is composed of various cohorts. Preliminary sensitivity tests showed that model outputs after 10 years are not sensitive to the number of individuals initially released nor to their random release location, except if the populations immediately collapse due to the absence of recruitment during the first year. Details about different environmental conditions used for the initialization are given in Section 2.3 of the main manuscript.

1.6 Input data

1.6.1 Fish data

Fish data input were the parameters of the bioenergetics model (see section 1.7.6), which can be considered as processed data because these parameters were estimated through the integration of numerous field data and in-situ observations.

1.6.2 Environmental data

The environmental input was the hindcast simulation from the coupled physical-biogeochemical model (ROMS-PISCES, Shchepetkin and McWilliams, 2005; Aumont and Bopp, 2006) of the study area with a horizontal resolution of ~8 km (1/12°) from 10°N to 35°N and 9°20'W to 23°W. The processes represented by ROMS-PISCES, in particular the spatio-temporal variability of the coastal upwelling and primary productivity act as a strong environmental forcing for the virtual fish population spatial dynamics and reproduction success. The forcings for this hindcast simulation are interannual time series reanalysis of wind, heat, solar and water fluxes over the period 1980-2009 (NCEP Climate System Forecast Reanalysis; Saha et al. 2010) and consistent boundary conditions from a NEMO-PISCES simulation of the North Atlantic basin at a lower resolution (1/4°; Tomas Gorgues, pers. comm.). We refer to Auger et al. (2015, 2016) for a complete description and validation of this hindcast configuration. Mean value and seasonal amplitude for surface temperature, phyto- and zooplankton simulated by this configuration are presented in Figure S14.

1.7 Submodels

1.7.1 Vertical motion

In the current form of the model, the vertical behavior is stage-dependent but does not include adaptation to environment (*e.g.*, thermocline or oxycline), with the exception of egg buoyancy following water density and bathymetric limitation for the maximum depth. Four different behaviors were defined for eggs, passive larvae, active larvae and juveniles or adults (Eq. 1). After spawning, eggs are uniformly distributed between 0 and 50m, and the effect of vertical currents is combined with eggs buoyancy. Eggs were considered positively buoyant with an excess buoyancy of 0.7 sigma-t in comparison to seawater surface density (Goarant et al. 2007). After hatching, larvae are considered passive until the absorption of the yolk-sac (thus, passively transported by vertical currents). Then, active larvae (age > 8 days) undergo vertical diurnal migrations from 0 to 60m (see Mbaye et al. 2015, for sensitivity tests on the diurnal vertical migration scheme). For juveniles (body-length > 5 cm) and adults, the vertical position in the water column was randomly picked from a Gaussian distribution centered on 30m at night and 10m during the day, with a width (sigma) of 10 m. This choice was based on acoustic observations from Brehmer et al. (2007).

$$\begin{cases} Z_{(t+1)} = W_{x(t)} \cdot dt + B_1(t) \cdot dt & (for\ eggs) \\ Z_{(t+1)} = DVM\ 0\text{-}50m & (for\ larvae) \\ Z_{(t+1)} = Gaussian(D,\sigma) & (for\ juvenile\ and\ adults) \end{cases} \quad Eq.1$$

1.7.2 Horizontal movement

For eggs and passive larval stages, the horizontal swimming movement is considered null, but a specific vertical motion is applied, which is affected by the horizontal current resolved for each layer. Once the body-length reaches 5cm, the horizontal swimming velocity was calculated following an extended kinesis algorithm (Eq. 2).

$$\begin{cases} X_{(t+1)} = U_{(x,y,z,t)} \cdot dt + V_{swim_1(t)} \cdot dt \\ Y_{(t+1)} = V_{(x,y,z,t)} \cdot dt + V_{swim_2(t)} \cdot dt \end{cases} \quad Eq.2$$

The relative importance of the swimming direction increases as the body length increases, because swimming speed is related to body length (Eq. 3). The kinesis algorithm was chosen because it takes as input the immediate environment of the fish rather than assuming a sensing of the distant environment, and because it was shown to perform best in very patchy environments (Watkins and Rose, 2013). In this form, it appeared that the algorithm did not perform well for the case of small pelagic fish in our coastal upwelling habitat (*i.e.*, with constant currents flushing away the individuals). A modification to Watkins and Rose (2013) was included to distinguish the cases when habitat quality improves from one time step to the other, inspired by the "extended" kinesis in Okunishi et al. (2012). This contributes to enhancing inertia in the movement algorithm. Finally, at each time-step, the horizontal swimming velocity components are calculated following (Eq.3):

$$\begin{cases} S_t = S_{t-1} & if \;\; Q_t > Q_{t-1} \\ S_t = f(S_{t-1}) + g(\theta) & if \;\; Q_t \leq Q_{t-1} \end{cases}$$

with

$$f(S_{t-1}) = S_{t-1} H_1 I_H$$
$$g(\theta) = \Phi \mathcal{E}(\theta)(1 - H_2 I_H) \qquad \text{[Eq. 3]}$$

where S_t is the computed velocity for time step t. H_1 and H_2 are the height for the inertial ("f"), random ("g") components, respectively set to H_1=0.6, H_2=0.9. $\boldsymbol{\Phi}$ is the maximum sustainable speed during one time step (see section 1.8.1 for the effect of values tested). θ is a random number from a normal distribution of mean $\sqrt{0.5\boldsymbol{\Phi}}$ and a standard deviation of 0.5Φ, and with a random sign. I_H is an index of the habitat quality evolution since the last time step (Watkins and Rose 2013; Eq. 4);

$$I_H = e^{-\left(\frac{\Delta Q}{\sigma Q}\right)^2} \quad \text{Eq. 4}$$

where ΔQ is the difference between the Habitat Quality Index (HQI; see Section 1.7.3) experienced at t and at t-1, and $\boldsymbol{\sigma}$Q a constant, which determines the threshold between an inertial or random swimming component (the smaller $\boldsymbol{\sigma}$Q, the fastest the swimming switch to the random component).

1.7.3 Habitat Quality Index

The HQI was defined following Watkins and Rose, 2013 for kinesis (Eq. 5):

$$Q = \delta + (1-\delta)G - \delta M \qquad \text{[Eq. 5]}$$

where G and M are respectively the spatial growth and mortality cue between 0 and 1; and δ represents the importance of G and M relative to HQI. For δ=1, HQI only relies on the mortality index, while for δ=0 HQI only relies on the growth index. For example, δ = 0.2 means that 20 % of the HQI depends on avoiding areas with high mortality index (due to predation or competition; see Section 2.3.3). In the preliminary runs, we tested the model sensitivity for δ=0; 0.25; 0.5; 0.75 and 1. Finally, the value of δ=0.2 was considered as sufficiently high in order to keep the majority of the individuals to remain over the continental shelf, and sufficiently low such that the temperature and food variability still impact significantly the total HQI (and thus generate migrations driven by these dynamic environmental parameters). The spatial growth index and mortality index are described in Sections 1.7.4 and 1.7.5.

1.7.4 Growth Cue

It is important for the reader to notice that the "growth cue" defined here following the terminology by Watkins and Rose, (2013) is used for Habitat Quality Index calculations (previous section), and thus for swimming behavior, but in the present model this growth cue does not directly impact the actual growth rate of the individuals, which is provided by the bioenergetics model (see Section 1.7.6). The Growth Index is defined as the product of the scaled food functional response *f* and the Temperature Preference Index:

$$G = TPI \times f \qquad \text{[Eq. 5]}$$

with f is given by (Eq. 6):

$$f = \frac{X}{X+X_k}$$ [Eq. 6]

where X is the concentration of carbon contained in plankton (simulated by ROMS-PISCES) encountered by the fish. X_k is the half-saturation constant set to 3 µmol C L^{-1}, so that in the coastal upwelling area food was generally non-limiting f > 0.8. This food proxy remains high all year round in the coastal area from 14 to 25°N but is more variable offshore and south of 14°N (Fig. S17).

The TPI is given by Eq. 7:

$$I_T = e^{-\frac{(T-T_{opt})^2}{2\sigma^2}} \qquad \sigma = log(\frac{Body\ \ length}{3})$$

(Eq. 7)

where T is the temperature simulated by ROMS and experienced by the fish (at the position of the individual). T_{opt}, the preferred temperature, was a key parameter that has strong impact on species distribution, but for which no observations at the individual scale are available. Thus we performed tests on the way to define T_{opt}, either as a constant for the species, following observations in the Senegal–Mauritania area (21°C; Fréon 1986) or as the temperature experienced when the individual was spawned as a mimic of *imprinting*, as suggested in the generalized natal homing theory (*e.g.*, Cury 1994). In both cases, the tolerance to variability around the preferred temperature was considered to increase as the body-length increase (Eq. 7).

1.7.5 Mortality Cue

The mortality experienced by individuals depends on their geographic position, their size and their age. In this section, we describe the spatial component that is used for Habitat Quality Index calculation (Section 1.7.3), and thus for swimming behavior. The actual mortality rate of the individuals also includes the size-dependent and age-dependent mortality (see Section 1.7.6). We hypothesised that the offshore predation mortality increases for *S. aurita*, which would be responsible for its absence out of the continental shelf, according to observations. The Mortality cue used was set to 0 on the shelf and 1 where bathymetry > 2000m (Fig. S18).

1.7.6 Bioenergetic model

The bioenergetic model used is the Dynamic Energy Budget (DEB; Kooijman, 2010). The energy intake is distributed into three compartments: the structure, the reserve and the maturation. The body-length is derived from the structure compartment using a specific shape coefficient. Here we assumed the same shape coefficient as the *Sardina pilchardus* for which a DEB configuration was already available (http://www.bio.vu.nl/thb/deb/). This allowed us to apply a simple body-size scaling relationship to adapt the fitted *Sardina pilchardus* DEB model to *S. aurita*. For this purpose, the maximum observed size is needed. The database of the CRODT was explored and revealed that the maximum observed size of *S. aurita* corresponded to several females collected in 1996 in Saint Louis, with total length > 44 cm (Mor Sylla, CRODT, pers. com). The DEB parameters obtained after applying the body-size scaling relationship are listed in Supplementary Table S1.

Table S1 : Specific parameters for the *S. aurita* DEB model adapted from the *Sardina pilchardus* configuration by applying a body-scale relationship.

Parameter	Unit	Value for *S. pilchardus*	Value for *S. aurita*
Maximum surface-specific assimilation rate (p_Am)	$J.d^{-1}.cm^{-2}$	1.0845e+03	1.6778e+03*
Maturity at birth (E_Hb)	J	1.372	1.2**
Maturity at puberty (E_Hp)	J	1.928e5	7.1394e5*
*: Zoom factor applied (z)= 1.547 (z^3 for E_Hp); ** E_Hb was set smaller for *S. aurita* since the size of the eggs are smaller than *S. pilchardus* (respectively diameters of 1.2 and 1.6 mm; Fontana, 1969; Coombs *et al*. 2004).			

The Arrhenius temperature correction function was chosen to define the correction factor applied to all the energy flux between the DEB compartments. A correction factor >1 means a faster metabolism needing more energy intake, while a factor <1 means slower growth and maturity but lower maintenance costs. The parameters for the Arrhenius temperature correction function were set according to a literature review of the most extreme temperatures were *S. aurita* were observed, which led us to apply a correction flux factor >0.5 for a temperature range of 12-30°C (Fig. S 3). Indeed, it appears that presence of *S. aurita* was reported in a very large range of temperature, from ~10°C in the Mediterranean Sea (Tsikliras and Antonopoulou, 2006) up to 29°C in Senegal (Marchal, 1991), in the Guinean Gulf (Quaatey and Maravelias, 1999; Pezenec and Bard, 1992) and in Venezuela (Rueda-Roa, 2012).

Spawning activity reported in surface waters ranged from 16°C in Senegal (Conand, 1977), 17°C on the Sahara Bank and in the Mediterranean Sea (Ettahiri *et al.* 2003; Sabates et al. 2006) to 29°C in Senegal (Marchal, 1991). The coldest gonadal development was observed in Greece at 15°C (Tsikliras and Antonopoulou, 2006), and the only report of massive *S. aurita* deaths related to temperature was also in Greece in 0°C water (Economidis and Vogiatzis, 1992). In Senegal, Boely et al. (1982) claimed that the preferred temperature for *S. aurita* was 18-20°C although they can be found in much colder or warmer water. Also in Senegal, Fréon (1988) found the preferred temperature was 21°C, while Marchal (1991) suggested the preferred spawning temperature ranged from 22°C to 25°C in May-June and from 28°C to 29°C in October-November. In the Caribbean, the highest *S. aurita* biomass was observed in surface waters at 25-27°C (Paramo et al. 2003; Rueda-Roa, 2012). In the Mediterranean Sea, Dulčić and Grbec (2000) reported *S. aurita* in 16-18°C waters in the Adriatic; and Palomera and Sabates (1990) described spawning activity near Spain in waters from 19° to 26°C. From *S. aurita* otolith analysis in Libya, Pawson and Giama (1985) found that spawning activity was not directly related to the temperature. For juvenile (until maturity), we considered a narrower range for temperature tolerance (correction flux > 0.5 for 15-27°C; Fig. S 3**Erreur ! Source du renvoi introuvable.**), as was suggested to be generally the case for teleost fish (Sogard, 1997).

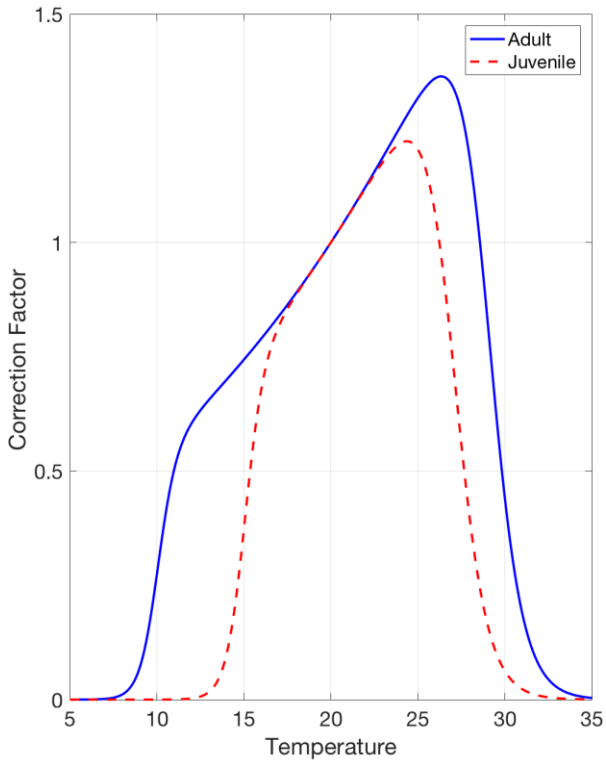

Fig. S 3: Temperature correction function for all energy fluxes used for Sardinella aurita. The upper and lower boundary were set in order to fit the extreme temperatures range in which S. aurita populations were observed.

The gonadal maturity cycle was set to conform to the description by Fontana (1969). Once individuals are mature, the energy previously allocated to development, can be allocated to the DEB reproduction compartment (buffer 1 in Fig. S 4). Once gonads are mature, egg batches begin to mature and are released (buffer 2 in Fig. S3). According to observations, the egg batches are released once a day (Conand, 1977). A limited number of batches can be released before the gonadal structure has to be rebuilt (state VII; Fontana, 1969).

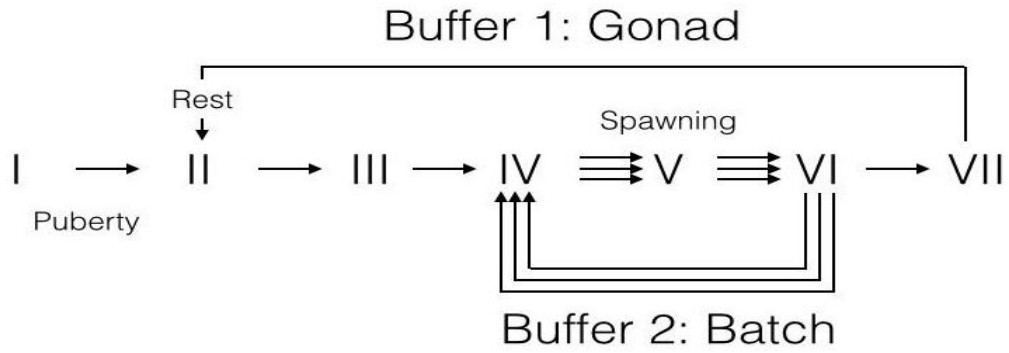

Fig. S 4: Illustration of round sardinella gonad dynamics model, following description by Fontana (1969).

1.7.7 Mortality Rate and Super Individuals Removal

There is two way for the SIs to finish their time in a simulation. First, the mortality rate reduces the worth of the SIs at each time step, and when the worth fall below 1000 (arbitrary threshold), the SI is removed from the simulation. This is the way natural predation mortality and fishing mortality are defined (size-dependent), as well as the senescence mortality (age-dependent). Second, the SIs can be removed from the simulation even if their worth is still high in two cases: (1) exit of the domain limits (happen often offshore and southward), or (2) starving occurs when the individuals' weight drops below 40% of the theoretical weight following the classical Von Bertalanffy growth statistical model for round sardinella.

For the natural predation mortality, the relationship to body-length translates the assumption that the larger the fish, the less potential predators may be encountered. Constant mortality rates were applied to eggs and passive larval stages, and then the mortality decreased exponentially as body-length increased (Fig. S 5: Daily mortality related to size dependent predation. The thresholds of 0.3 and 2cm were used to define respectively eggs stage and yolk-sac larvae (passive).), as described by Okunishi et al. (2012). Thus, the faster the growth, the lower the cumulative predation mortality. For example, under constant conditions (of T=18°C and f = 0.8), 99.3% of the individuals of a cohort die from predation between spawning to recruitment (10 cm, at 84 days). With a slightly higher temperature (19°C), this proportion lower to 99% due to faster growth (10 cm, at 74 days). Furthermore, a bathymetry-dependent correction factor, equal to 1 minus the mortality cue, was applied to reduce fish body-length before the calculation of the size-dependent mortality. As a result, SIs that move offshore have an increased predation mortality.

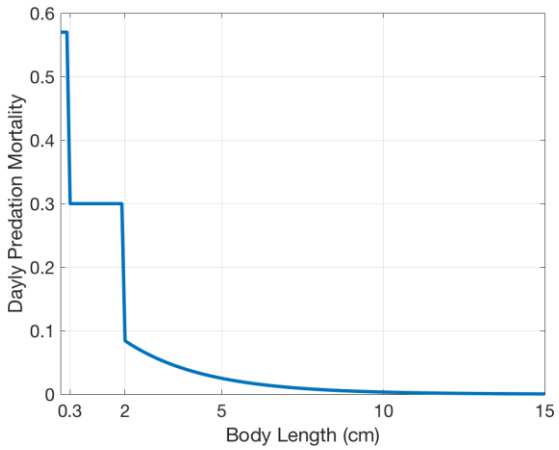

Fig. S 5: Daily mortality related to size dependent predation. The thresholds of 0.3 and 2cm were used to define respectively eggs stage and yolk-sac larvae (passive).

The fishing mortality (F) was considered for fish larger than 12 cm (the smallest size found in the round sardinella landings in Senegal) and was set to 1.4 year^{-1}, applied at a daily rate to the "worth", or number of fish represented by the SI (daily fishing mortality F = 0.0038 day^{-1}). This resulted in an average SI longevity of 4.5 years.

The daily senescence mortality (Sm) was defined by Eq. 9. The associated daily mortality is 0.01% at 5 years and ~1% at 10 years. This results in a maximum lifetime of about 12 years for a SI in ideal conditions, and an average longevity of 6.5 years for the SI exposed to the virtual environment provided by the ROMS-PISCES configuration. This fits longevity estimations derived from otolith analysis for *S. aurita* in other real environments,

thus including fishing mortality (7 years; Chescheva, 2006 and Gaamour *et al.* 2003). Spatio-temporal changes in fishing mortality were not included in the model.

Sm = 10^{-12} x (age in day)^3 (Eq. 9: daily senescence mortality**)**

1.8 Simulation experiments

1.8.1 Preliminary Sensitivity runs

During the onset of the model and debugging phase, a large number of simulations were performed. In particular, the parameters of the adult movement were of particular importance given that we wanted to allow the emergence of migration patterns. These numerous simulations (>100) are not presented, but they allowed to fix the parameters' values (see Table S2).

Table S2 : Summary list of model parameters

Submodel	Parameter symbol	Value tested	Explanation
Fish movement algorithm (Kinesis)	Phi	3, 4, 4.5, 6	Maximum allowed swimming speed during one time step
	H1	0.6	Height of the inertial component
	H2	0.9	Height of the random component
	σQ	0.13	Sharpness of the switch between random and inertial components
	δ	0, 0.2, 0.25, 0.5, 0.75, 1	Weight of the Mortality vs. Growth cues in the Habitat Quality Index
	dt	10, 20, 60, 120 min	Time step
DEB model	E_init	2.58 J	Initial Reserve (Joules)
	V_init	10^{-6} cm^3	Initial volume (egg)
	T_L	10 (15) °C	Lower boundary tolerance range for adult (juvenile)
	T_H	29 (27) °C	Upper boundary tolerance range for adult (juvenile)
	T_ref	20°C	Reference temperature
	T_A	5000 K	Arrhenius temperature
	T_AL	50000 K	Arrhenius temperature for lower boundary
	T_AH	190000 K	Arrhenius temperature for upper boundary
	p_Am	1.4980e+03 $J/cm^2/d$	Maximum surface-specific assimilation rate

	F_m	6.51 l/d.cm^2	Maximum specific searching rate
	kap_X	0.8	Digestion efficiency of food to reserve
	v	0.1379 * 2.4019 cm/d	Energy conductance
	Kappa	0.3436	Allocation fraction to soma = growth + somatic maintenance
	kap_R	0.95	Reproduction efficiency
	p_M	92.51 J/d.cm^3	Volume-specific somatic maintenance
	p_T = 0	0 J/d.cm^2	Surface-specific somatic maintenance
	k_J	0.002 d^{-1}	Maturity maintenance rate coefficient
	E_G	4767 J/cm^3	Specific cost for structure
	E_Hh	1 J	Maturity at hatching
	E_Hb	0.8 J, 1.2 J	Maturity at birth
	E_Hj	20 J	Maturity at metamorphosis
	E_Hp	5.0813e+05 J	Maturity at puberty
	del_M	0.1391	Shape coefficient
	d_V	0.2 g/cm^3	Specific density of structure (dry weight)
	mu_V	500000 J/mol	Specific chemical potential of structure
	mu_E	550000 J/mol	Specific chemical potential of reserve
	w_V	23.9 g/mol	Molecular weight of structure
	w_E	23.9 g/mol	Molecular weight of reserve
	c_w	1 - d_V	water content (c_w * W_w = total water weight)
Habitat Quality Parameters	Topt	21°C, natal temperature	Optimal temperature tracked by individuals
	X_K	3, 6 µmol C L-1	Food concentration for half saturation of the response function
Spawning parameters	Rel_fec	400 egg/g	Relative fecundity for S. aurita (Fréon 1988)
	nbeggs_max_per_SI	10^{10} eggs	Maximum number of eggs per new super individual
Early life parameters	Spawn_depth	50m	Maximum depth for the eggs release
	egg_duration	1 day	Time before hatching
	YolkSacLarvae_duration	8 days	Time between hatching and start of the diurnal vertical migration

	Swim_lowerlimit	50m	Maximum depth for the diurnal vertical migration
	bathy_max	200m	Threshold isobath for the larval retention test
	Age_min	30 days	Age at which the larval retention criterion is assessed
	nrec_max_day	1	Maximum number of newly recruited SI per day
Mortality	F_annuel	0, 1.4, 3, 4	Annual fishing mortality
	Rec_size	10, 12 cm	Minimum body-length for the fishing mortality

We tested for maximum swimming speed values between 3 to 6 BL/s (Body-length per second), and found that 4 BLs was a threshold value under which the SI seasonal migrations could not cross the Cape Blanc area (21°N) during their northward migration. By contrast, for values higher or equal to 4 the northward migration reach ~26°N

We also tested the effect of different intensity of the offshore predation. This strongly impacted the offshore extent of the population. Indeed, when considering no offshore mortality (delta =0 in the HQI, Eq. 4) a large number of individuals remained trapped in mesoscale structures as eddies and filaments carrying high food concentration far offshore during the upwelling season. A large part of the SIs followed these structures offshore until they reached the western limit of the domain (30°W), or they settled around the Cape Verde islands when the eddies get trapped. This strongly altered the size of the virtual population, which maintained itself only in the area around the Arguin Bank. Although the Cape Verde fisheries institute confirmed the sporadic presence of *S. aurita* in the eastern islands (annual report of INDP, 2012), to our knowledge observations of *S. aurita* beyond the continental shelf were never reported by scientific R/V. This effect could not be fixed by increasing the food half-saturation constant. Thus, for the rest of the simulations we considered delta = 0.2, *i.e.* a behavior of avoidance of offshore predation based on bathymetry.

1.8.2 Selection of the correct set of serial simulations

Sensitivity runs were performed upon HQI parameters and fish swimming velocity (Table 1 of the main text), presented in Section 2.3 of the main manuscript.

2 - Supplementary Figures of the Environmental Forcings

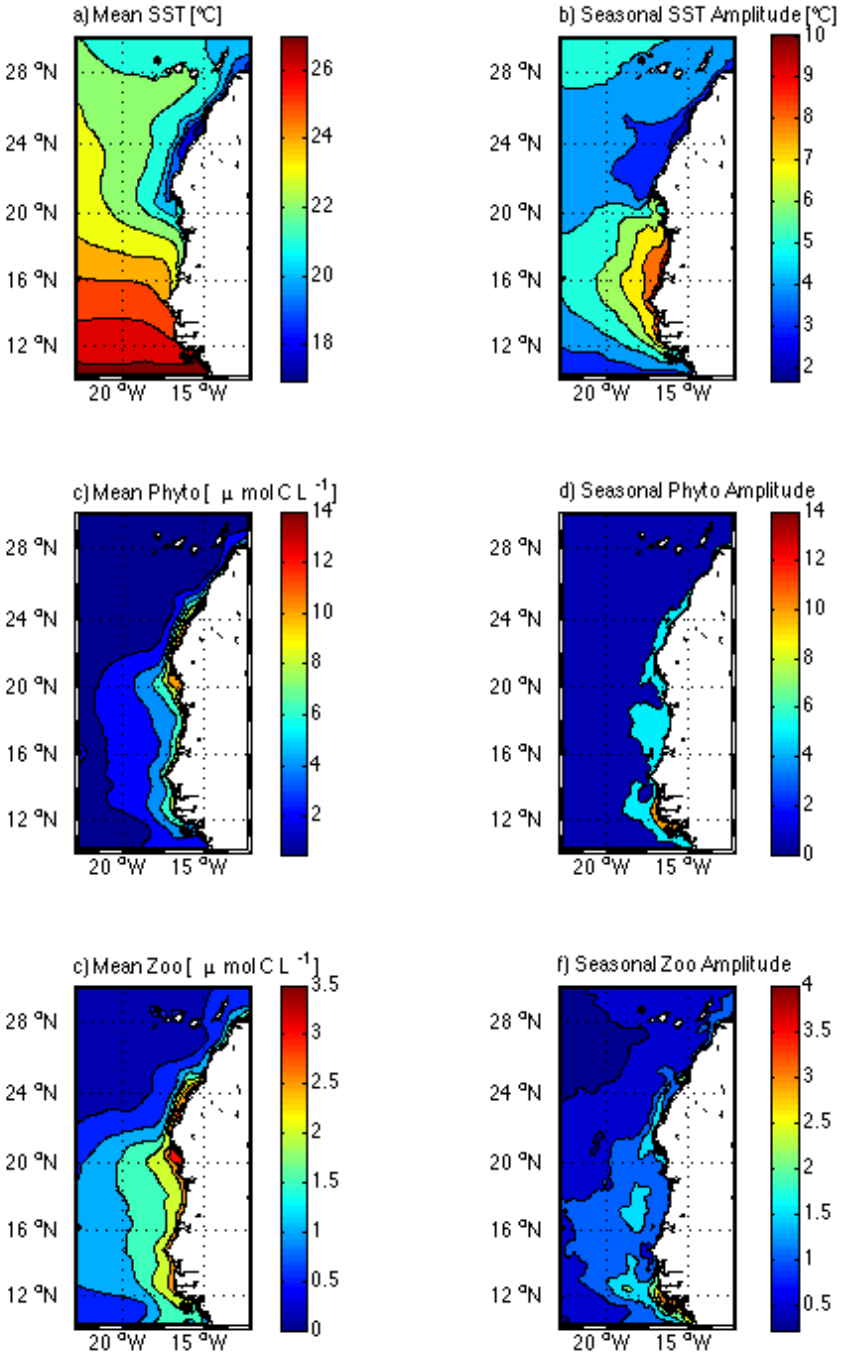

Fig. S 6: Mean values and seasonal amplitude for (a, b) surface temperature, (c, d) surface phytoplankton and (e, f) surface zooplankton. Averages from 1990 to 2009 ROMS-PISCES simulation (Auger et al. 2015).

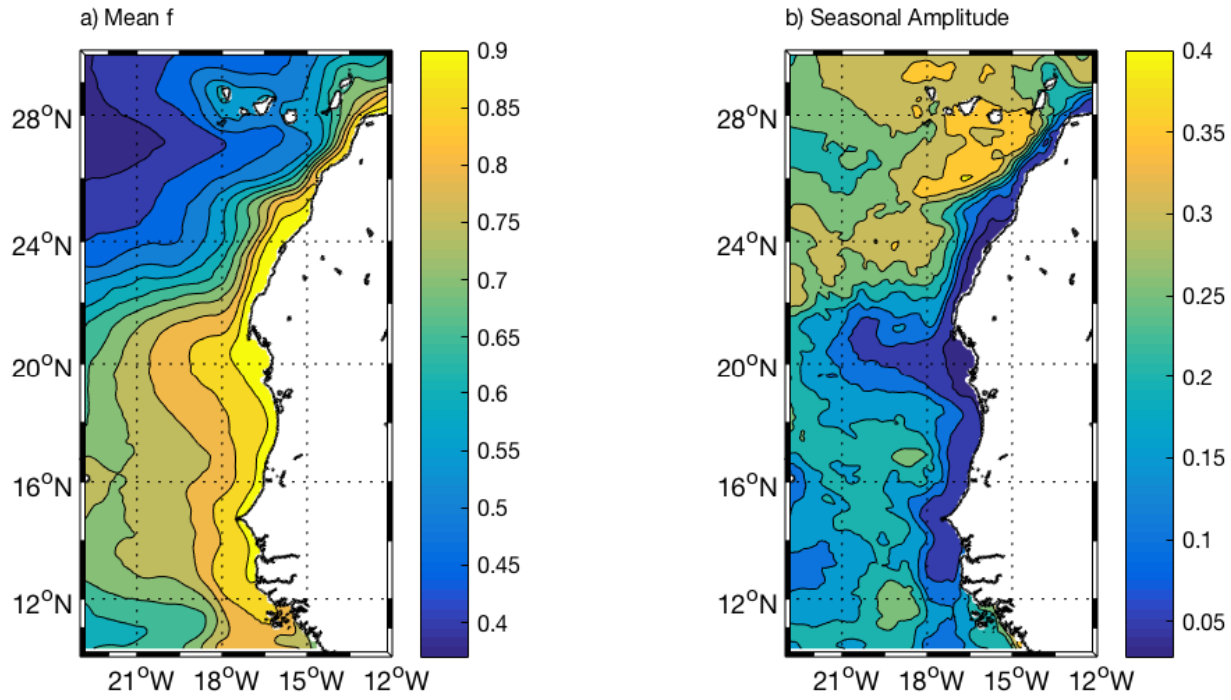

Fig. S 7 : Mean food functional response (a) and seasonal amplitude (b), using total phyto- and zooplankton carbon as food proxy, with a half-saturation constant of 1 mg C·L-1. Average from 1990 to 2009 ROMS-PISCES simulation (Auger et al. 2015).

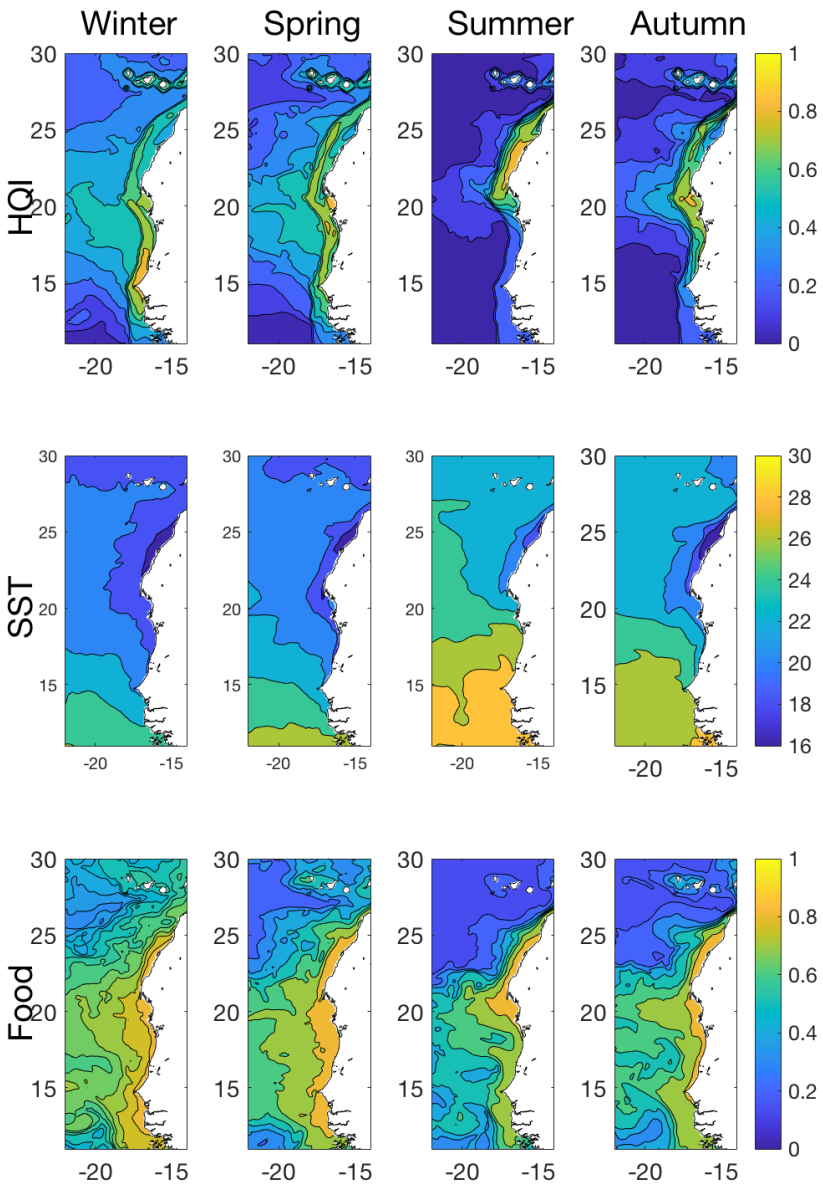

Fig. S 8: Seasonal climatology of the Habitat Quality Index (HQI) for a preferred temperature of 21°C (top), surface temperature (middle) and food functional response (bottom). Columns 1-4 correspond to seasons 1 to 4, respectively. For the temperature, the filled areas correspond to 2°C intervals from 16-18°C (dark blue, in the coastal area north of 24°N) to 28-30°C (yellow, south of 15°N at season 3). HQI and food functional response ranges from 0 (blue) to 1 (yellow).

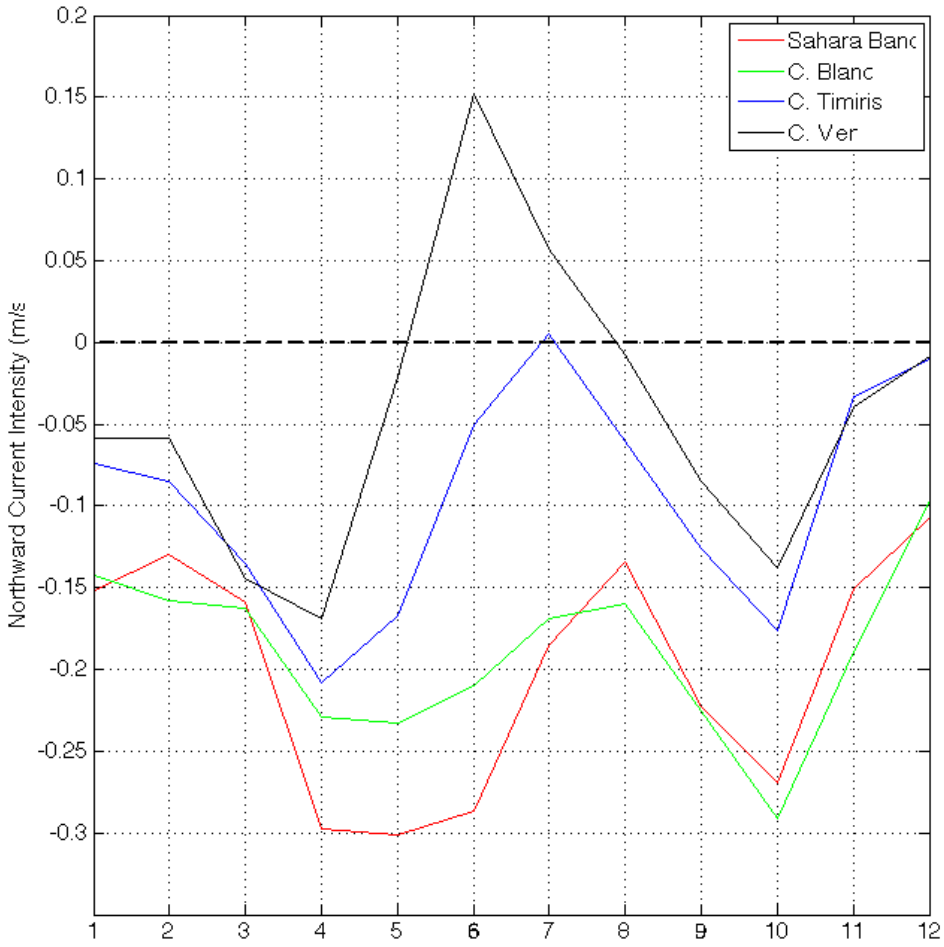

Fig. S 9: Average monthly northward current (m/s) resulting from the 'ROMS' Regional Ocean Modeling System during the 1990-2008 period at locations in the Sahara Bank (21°N - 17.5° W), Cape Blanc (21.5N, 17.5W), Cape Timiris (19.3N, 16.6W) and Cap Vert (14.7 N - 17.5 W). Negative values correspond to southward flowing currents.

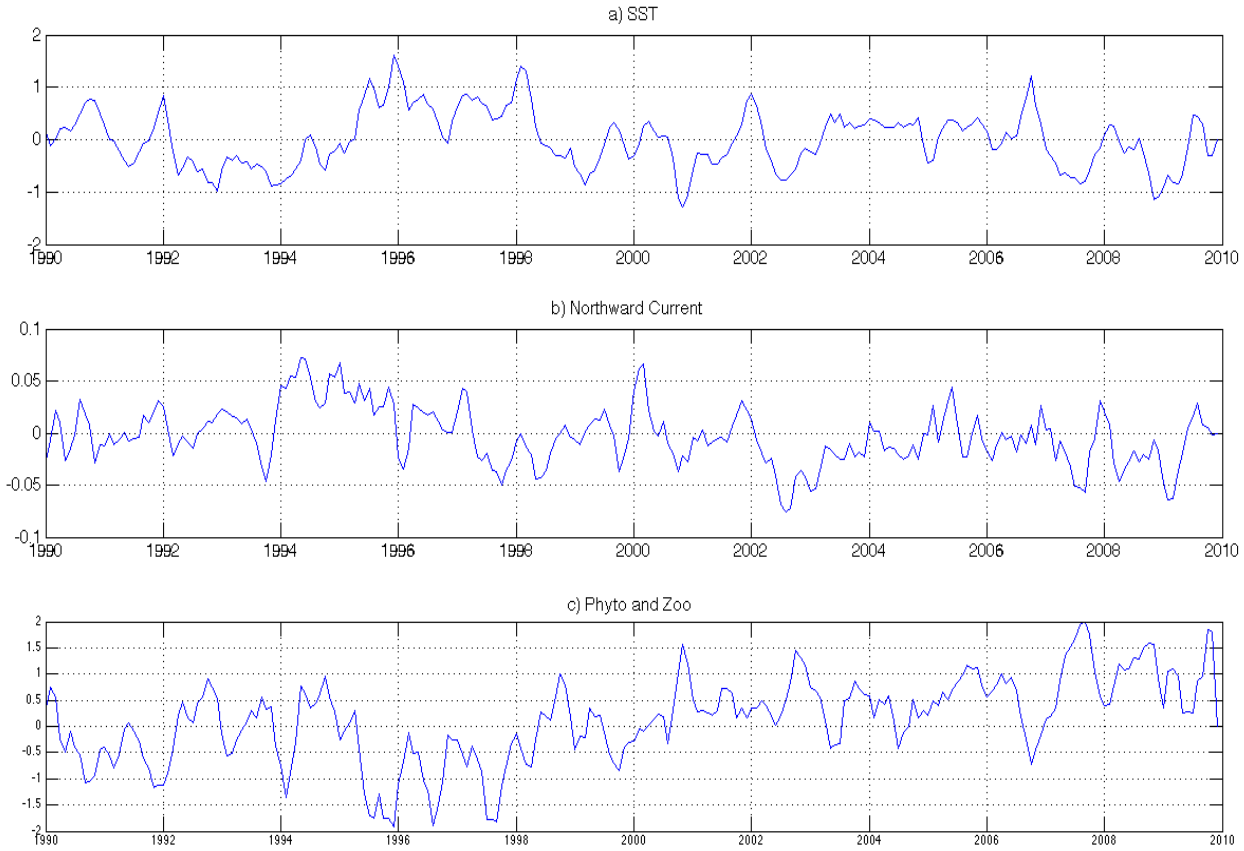

Fig. S 10: Time series of anomalies over the Sahara Bank (21-26°N) for a) sea surface temperature (°C), b) average northward current (m/s), and c) combined phyto- and zooplankton concentration (µmol C L-1). The two last panels correspond to averages in the upper layer (0-30m).

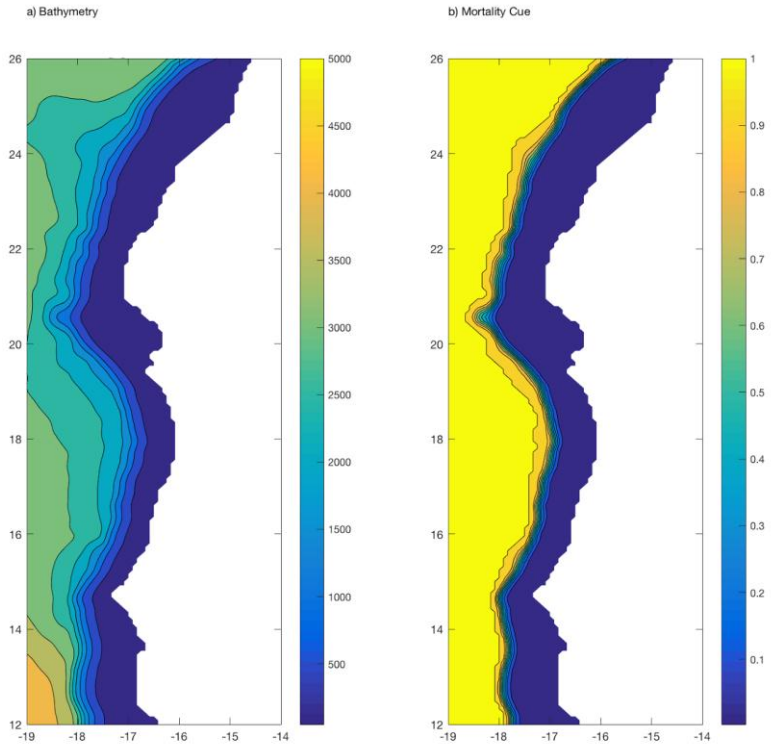

Fig. S 11 : Bathymetric map used in the ROMS-PISCES simulation (a) and mortality cue derived from bathymetry in order to represent the increased offshore predation (b).

2 - Supplementary Results

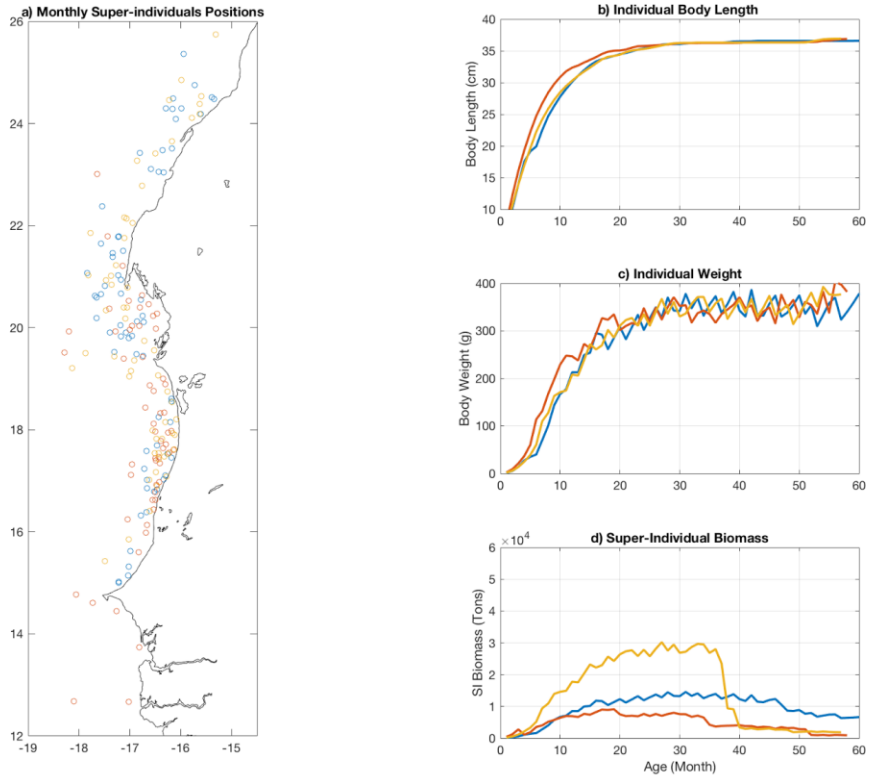

Fig. S 12: Monthly positions (a), individual body length (b), individual weight (c) and total biomass represented by three super-individuals randomly selected among the ones performing migrations from south of 14°N to north of 21°N. (Each color corresponds to one super-individual.)

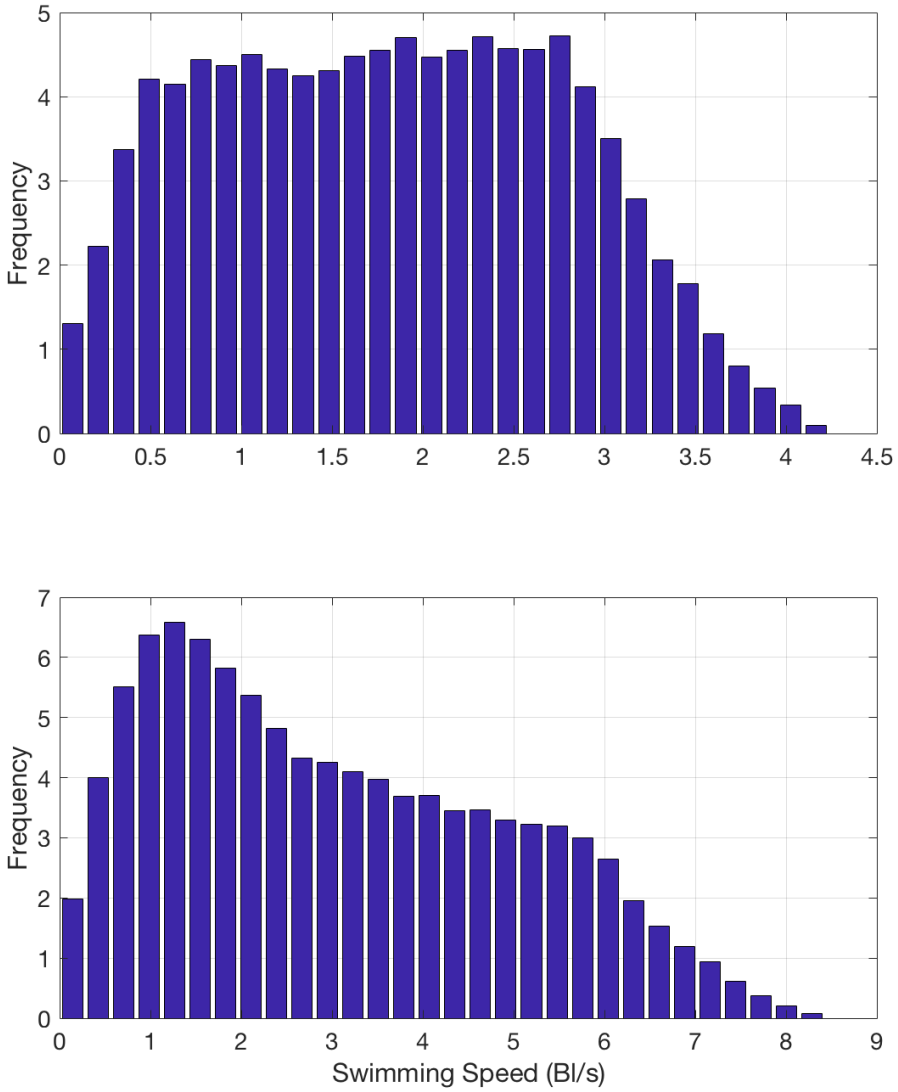

Fig. S 13: Distribution of individuals' instantaneous velocities in the case of Φ = 3 BLs-1 (top) and Φ = 6 BLs-1 (bottom), from monthly snapshots of the individuals' velocity (BLs-1 = Body lengths per second).

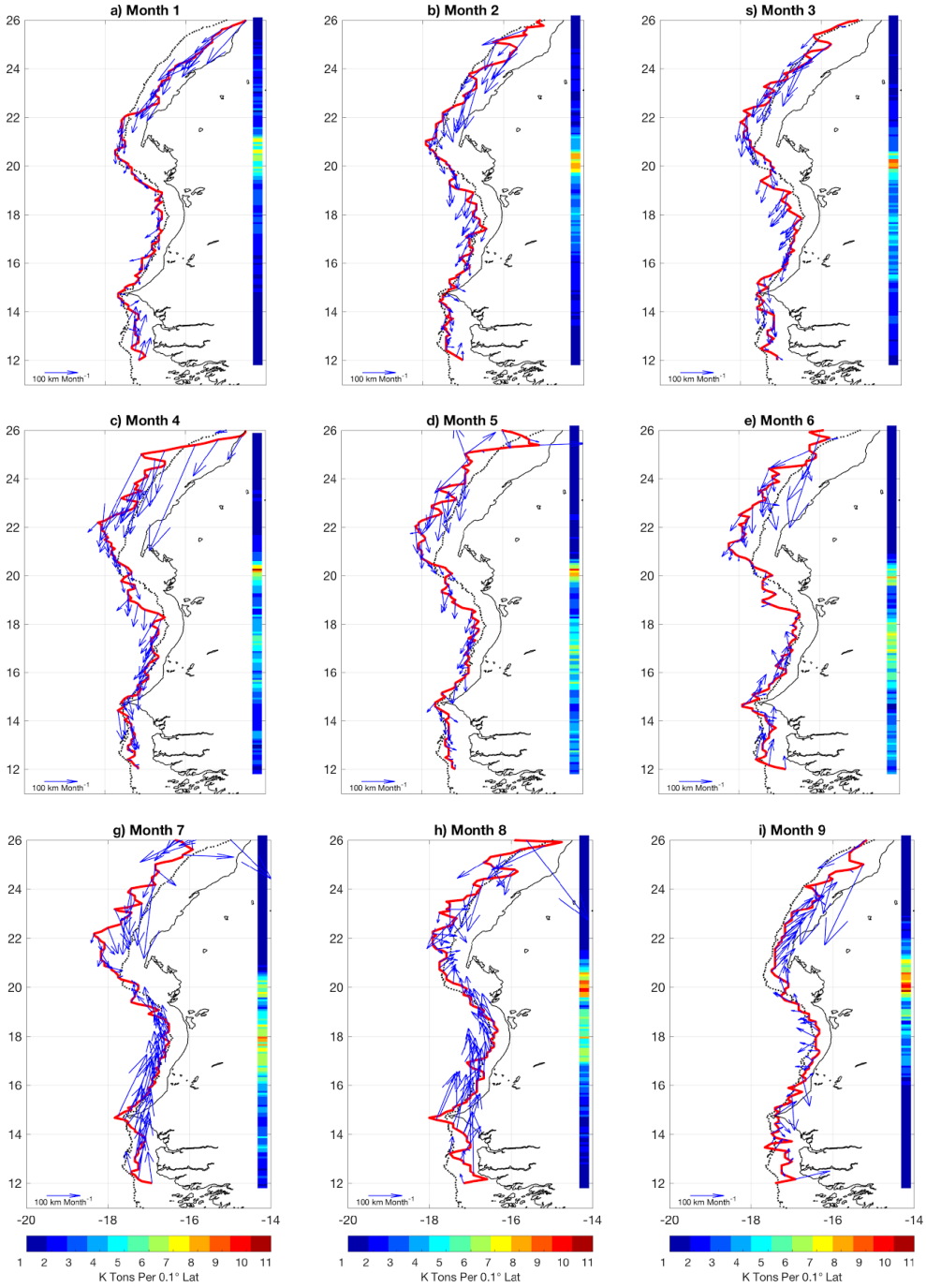

Fig. S 14: Monthly average spatial distribution and movement. Arrows show average movements (direction and intensity). The vertical color bars indicate latitudinal fish density distribution (1000 Tons per 0.1° latitude). A thick red line highlights the limit of the offshore extent of the fish biomass, and the black dashed line is the 200 m isobath.

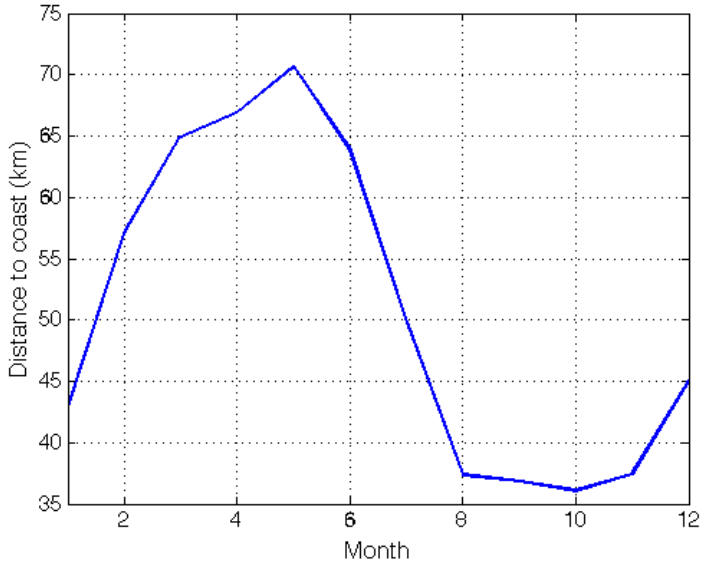

Fig. S 15: Monthly distance to coastline that includes 50% of the round sardinella adult biomass.

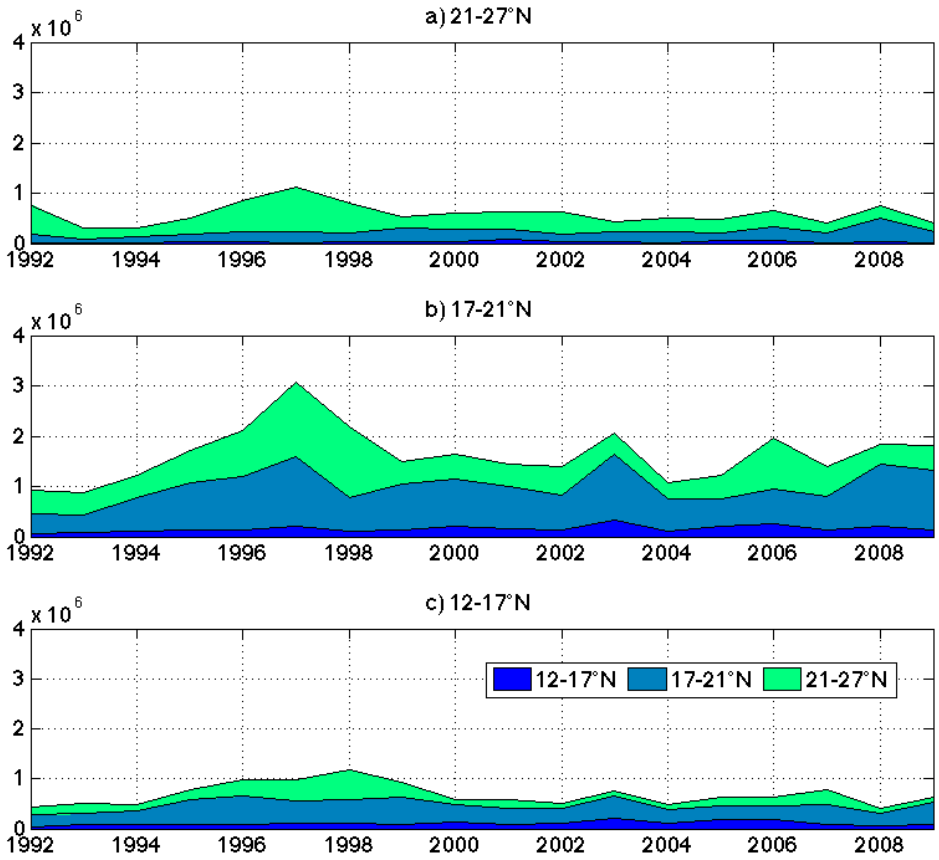

Fig. S 16: Simulated interannual variability in round sardinella biomass predicted by the model (Simulation 2). The colored area shows the contribution of each nursery area to the total variability. Note the large contribution of the recruitment in Morocco and Mauritania (top two panels). Recruitment in Morocco was mainly responsible for the regional biomass increase from 1995 to 1999.